Experimental investigation of boundary condition effects in bipennate fluidic artificial muscle bundles

Hart, Rebecca, Duan, Emily, Bryant, Matthew

Rebecca Hart, Emily Duan, Matthew Bryant, "Experimental investigation of boundary condition effects in bipennate fluidic artificial muscle bundles," Proc. SPIE 12041, Bioinspiration, Biomimetics, and Bioreplication XII, 1204108 (20 April 2022); doi: 10.1117/12.2615896

Event: SPIE Smart Structures + Nondestructive Evaluation, 2022, Long Beach, California, United States

Experimental Investigation of Boundary Condition Effects in Bipennate Fluidic Artificial Muscle Bundles

Rebecca Hart[a], Emily Duan[a], Dr. Matthew Bryant[a]
[a]Department of Mechanical and Aerospace Engineering, North Carolina State University, Raleigh, USA

ABSTRACT

In this study, the implementation and performance of bipennate topology fluidic artificial muscle (FAM) bundles operating under varying boundary conditions is investigated and quantified experimentally. Soft actuators are of great interest to design engineers due to their inherent flexibility and potential to improve safety in human robot interactions. McKibben fluidic artificial muscles are soft actuators which exhibit high force to weight ratios and dynamically replicate natural muscle movement. These features, in addition to their low fabrication cost, set McKibben FAMs apart as attractive components for an actuation system. Previous studies have shown that there are significant advantages in force and contraction outputs when using bipennate topology FAM bundles as compared to the conventional parallel topology[1]. In this study, we will experimentally explore the effects of two possible boundary conditions imposed on FAMs within a bipennate topology. One boundary condition is to pin the muscle fiber ends with fixed pin spacings while the other is biologically inspired and constrains the muscle fibers to remain in contact. This paper will outline design considerations for building a test platform for bipennate fluidic artificial muscle bundles with varying boundary conditions and present experimental results quantifying muscle displacement and force output. These metrics are used to analyze the tradespace between the two boundary conditions and the effect of varying pennation angles.

Keywords: pennate topology, soft actuators, fluidic artificial muscles, muscle topology, bioinspired

1. INTRODUCTION

Biological systems offer superior functional performance and high adaptation capabilities when compared with traditional mechanical actuators[2]. For this reason, engineers and scientists often look to biological systems for inspiration when designing actuation systems. McKibben fluidic artificial muscles (FAMs) are hydraulic or pneumatic actuators that exhibit behavior akin to natural muscle contraction.

McKibben artificial muscles are constructed from dense helically braided mesh surrounding a soft inner bladder and offer the benefits of low fabrication cost, flexibility, and a high force to weight ratio. In application, these soft actuators offer an attractive improvement to efficiency and safety metrics in human-robot interactions. When compared to biological skeletal muscle, McKibben artificial muscles can achieve higher force outlets and higher strain rates which make them ideal high power actuators[3]. Thus, extensive research on McKibben artificial muscles has led to a well-established theoretical understanding of the output force, contraction, efficiency, and effects of braid angle variation[4–7].

In biological systems, muscle tissues are seen to have varying architectures. Most notably, the parallel configuration which is seen in the biceps brachii located in the bicep and a bipennate configuration seen in the rectus femoris in the quadricep. In the parallel muscle tissue topology, the muscle fibers are aligned with the direction of muscle contraction, while in the bipennate topology, the muscle fibers are symmetrically angled with respect to the muscle contraction direction.

These natural muscle architectures enable the human body to achieve specific tasks in an efficient manner. Therefore, we wish to draw inspiration from these characteristics when designing soft actuators. McKibben artificial muscles are characterized by their ability to replicate the mechanical behaviors seen in natural muscles. This characteristic has led to a heavy focus on biologically inspired design. This inspiration has led to McKibben artificial muscles being grouped into bundles to improve overall force output and efficiency[5,8,9]. Similar to natural muscle tissues, McKibben actuator bundles are composed of multiple actuation units. Each of these units is a single McKibben actuator which will be referred to as a

Bioinspiration, Biomimetics, and Bioreplication XII, edited by Raúl J. Martín-Palma
Mato Knez, Akhlesh Lakhtakia, Proc. of SPIE Vol. 12041, 1204108
© 2022 SPIE · 0277-786X · doi: 10.1117/12.2615896

muscle fiber. The collection of these muscle fibers will construct a McKibben muscle bundle referred to generally as a muscle bundle.

An analytical study compared pennate topology with parallel topology McKibben muscle bundles and concluded that there could be improvements of 2.2% in muscle bundle contraction and 2.7 times force generation when implementing a pennate bundle architecture within a bounding volume of the same dimensions as that of a parallel topology[1]. The bipennate architecture is composed of muscle fibers whose axis of contraction is at an angle to the direction of motion of the muscle bundle. In this configuration, muscle fibers experience rotation in addition to axial contraction and radial expansion. Previous studies have developed a kinematic model which relates muscle bundle outputs to muscle fiber inputs as a function of pennation angle and have demonstrated a proof-of-concept for pennate topology[10]. In an investigation on how to practically design pennate muscle bundle configurations given an operating volume, a model was constructed to predict force, contraction, stiffness, and work output[1]. The suggested future work from this previous study includes exploring varying design cases and implementing them in hardware[1]. In this paper, we wish to explore various design cases by varying the boundary conditions imposed within a pennate topology muscle bundle.

A boundary condition is defined as the way that the muscle fibers interact with their mounting points and neighboring fibers within the bundle. One way to bound the muscle fibers in a pennate configuration is to pin the fiber ends with fixed separation distances between neighboring fiber ends. This allows muscle fiber axial contraction, radial expansion, and rotation while including sufficient gaps between neighboring muscle fibers such that they do not contact one another during actuation and therefore do not mechanically interact. The second boundary condition considered here is inspired by the function of the connective tissue seen in biological muscles and is referred to as the “constant fiber contact condition”. This condition prescribes that neighboring muscle fibers always remain in contact during actuation and thus allows mechanical interaction among the muscle fibers and requires that the fiber end spacings vary during actuation.

The focus of this study is to experimentally determine the effects of the pennation angle and imposed boundary condition on the performance of a McKibben muscle bundle. This paper will outline the two boundary conditions, pinned and constant fiber contact, the key design components to be considered when implementing the boundary conditions in hardware, and the results of experimental testing of the bipennate fluidic artificial muscles.

2. PENNATE MUSCLE BUNDLE TOPOLOGY AND BOUNDARY CONDITIONS

2.1 Muscle bundle architecture and boundary conditions

A bipennate muscle bundle topology consists of one or more symmetrical muscle fiber pairs oriented around a center axis. The first muscle fiber pair is shaded green in Figure 1 while the other pairs are shaded blue**.** McKibben actuators in bipennate muscle bundle topologies undergo rotation in addition to radial expansion and axial contraction. This rotation is quantified by the pennation angle which is defined as the angle of the muscle fiber to the direction of actuation of the muscle bundle as pictured in Figure 1. The initial pennation angle is defined as the angle at which the muscle fibers sit when unpressurized with no applied load. This pennation angle will increase as the muscle fibers are inflated, up to an upper bound of 90°. If the muscle contraction is sufficient to reach this upper bound, the muscle fibers no longer contribute to the force and contraction output of the muscle bundle because there is no force produced in the direction of motion. In this case, the length of the contracted muscle fiber would be equal to the thickness of the muscle bundle and the height would be equal to zero. The thickness of the muscle bundle is defined as the horizontal distance between the ends of a muscle fiber; the height is defined as the vertical distance between the ends of a muscle fiber.

The focus of this study is to explore the effects of varying the fiber boundary conditions, specifically comparing the pinned boundary condition and the constant fiber contact boundary condition.

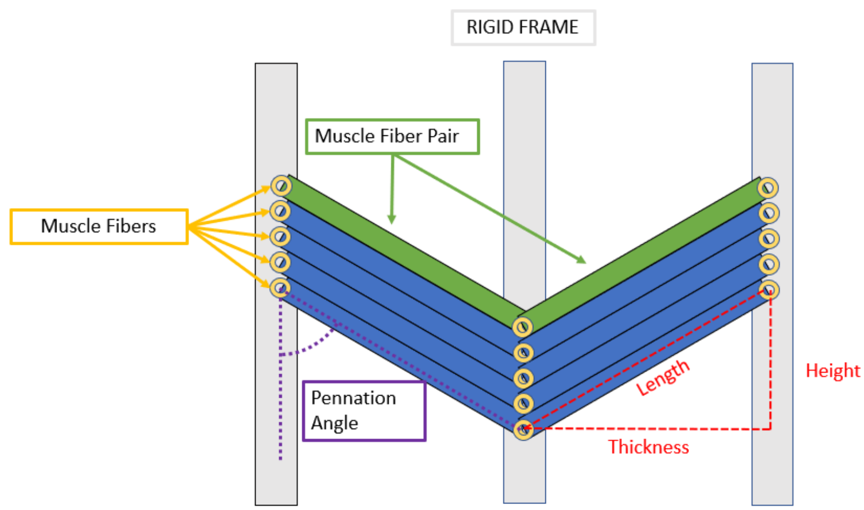

Figure 1. Two-dimensional representation of bipennate muscle bundle with fiber geometry parameters labeled.

2.2 Pinned boundary condition

The pinned boundary condition is a constraint for bipennate muscle bundle topologies where the muscle fiber ends maintain fixed separation distances and are free to pivot about a pin joint. This condition can be achieved by pinning one end of each muscle fiber to an outer rigid frame while the inner end of the muscle fiber is allowed to translate vertically (e.g. via a slider riding in a vertical guide) to actuate the load. The load is applied from the top of the muscle bundle in the direction which opposes the direction of motion during actuation. Both the inner and outer ends of the muscle fibers are evenly spaced throughout the actuation process. The spacing should be sufficient so that muscle fibers that have achieved maximum radial expansion are not in contact with other muscle fibers in the muscle bundle.

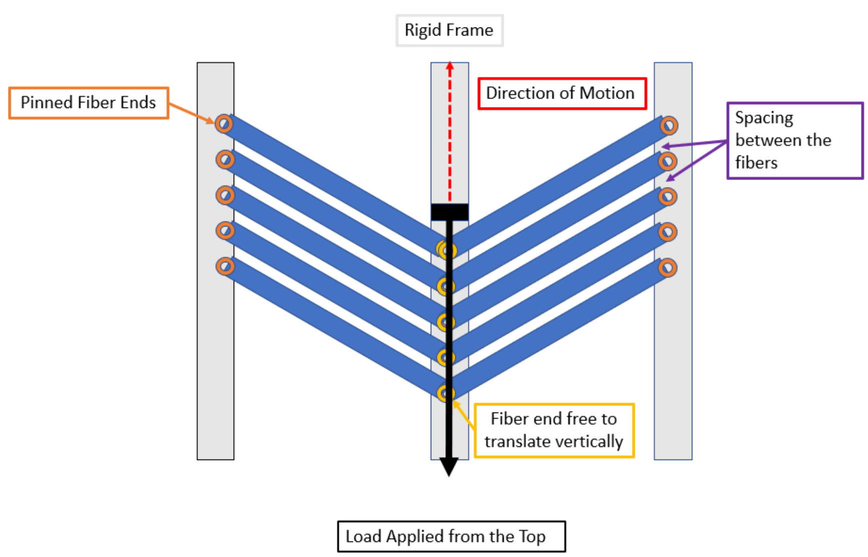

Figure 2. Two-dimensional representation of bipennate muscle bundle with a pinned boundary condition

2.3 Constant fiber contact boundary condition

The constant fiber contact constraint is a biologically inspired configuration intended to approximate the functionality of the connective tissue seen in natural muscles. To achieve this, the muscle fibers must remain in contact during contraction and the ends of the muscle fiber are allowed to slide relative to one another and are free to translate vertically. As the muscle fibers expand radially, both ends are free to slide in the same direction as the motion of the muscle bundle. The bottom pair of muscle fibers will be constrained to a minimum vertical position (e.g. by a stopper) to direct all vertical translation from radial expansion in the direction of motion of the muscle bundle. In the constant fiber contact boundary condition, the load is applied from the top pair of muscle fibers in the direction which opposes the motion during actuation. During the actuation process it is assumed that each muscle fiber remains perfectly cylindrical.

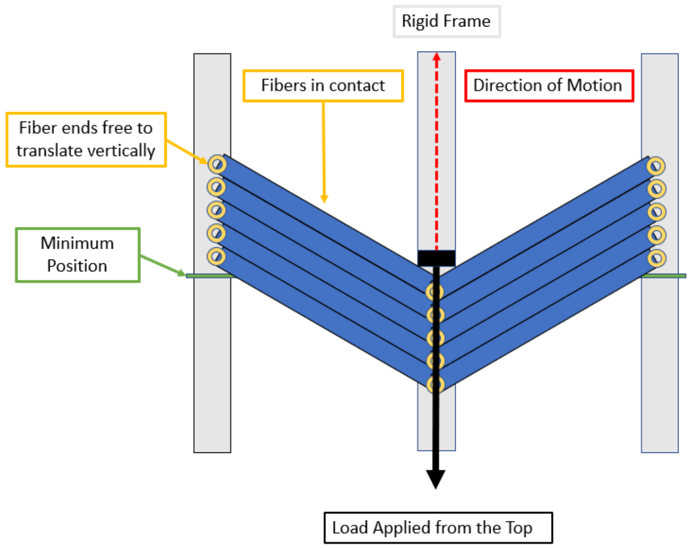

Figure 3. Two-dimensional representation of bipennate muscle bundle with a constant fiber contact boundary condition.

3. EXPERIMENTAL SETUP

In order to implement the boundary conditions described in Section 2 in hardware, the following design requirements were defined:

To achieve the pinned boundary condition:

1) The inner muscle fiber ends are pinned to guides that are allowed to translate vertically but maintain constant vertical separation distance between fiber ends
2) The outer muscle fiber ends are pinned to the fixed outer frame and are not allowed to translate vertically
3) The muscle fibers are allowed to rotate about their pins at both ends
4) The muscle fibers do not come in contact with each other during muscle bundle contraction

To achieve the constant fiber contact boundary condition:

1) The inner muscle fiber ends are pinned to guides that are allowed to translate vertically and can change the vertical separation distance between fiber ends
2) The outer muscle fiber ends are pinned to guides that are allowed to translate vertically and can change the vertical separation distance between fiber ends, but are limited to a minimum vertical position which facilitates the creation of the initial pennation angle
3) The muscle fibers are allowed to rotate about their pins at both ends
4) The muscle fiber surfaces will be in contact with the surrounding muscle fibers during muscle bundle contraction

A general experimental setup was designed to realize both boundary conditions in hardware. The test bed is able to accommodate the requirements of both the pinned and the constant fiber contact boundary condition by adding spacers and locking collars to satisfy the requirements of the pinned condition or removing them to facilitate the constant fiber contact boundary condition.

3.1 Vertical translation mechanism

Vertical translation is required along the central carriage for all bipennate boundary conditions. The constant fiber contact condition requires that both ends of the muscle fiber be allowed to translate freely. To achieve these constraints, carriages are constructed for each muscle fiber to ride along linear motion rods. These carriages are equipped with linear ball bearings to facilitate smooth vertical translation with minimal friction. The linear bearing carriages (seen in figure 4) are implemented on both muscle fiber ends and equipped with a different attachment mechanisms to be used for each end of the muscle fiber.

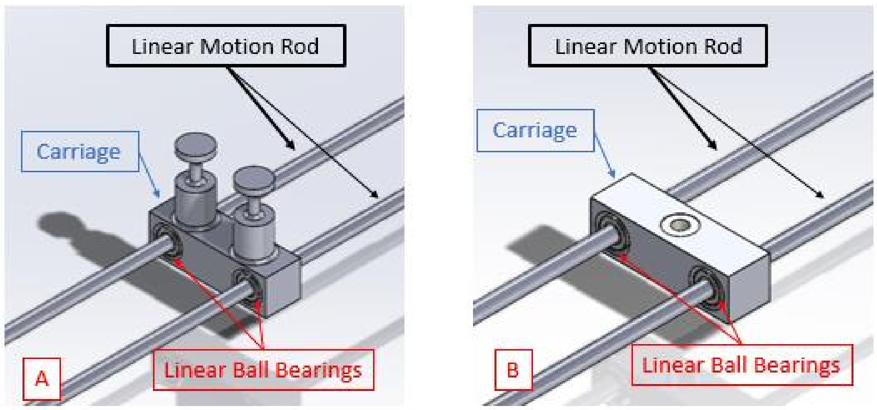

Figure 4. Linear bearing carriages equipped with linear ball bearings and pressed into a bearing housing. The bearing housings are modified to allow connection for each fiber end (A) used to attach the plugged fiber end (B) used to attach the inlet fiber end

3.2 Rotation mechanism

The defining feature of pennate topology is the muscle fibers' ability to rotate. FAMs are constructed with one end being plugged and the other end supplying the working fluid required for actuation. Both ends must be allowed to rotate freely and have fluid-tight seals. However, the varying hardware on the plugged and inlet ends of the muscle fiber present different challenges to integrating a rotational mechanism to the muscle fiber.

The inlet of a FAM is composed of a clear masterkleer soft PVC plastic tubing pressed into a latex bladder surrounded by braided mesh. To enable smooth rotation at the inlet end of the FAM, a sleeve bearing interfacing with a rotary shaft is used. The sleeve bearing, which is pressed into the sliding carriage, allows the FAMs to rotate with reduced friction in the system. The rotary shaft is pressed into a 3D printed housing. This housing is attached to the FAM using zip-ties. The zip-ties serve a dual purpose in this application to create a fluid-tight seal at the inlet and attach the mechanism needed to achieve rotation to the FAM.

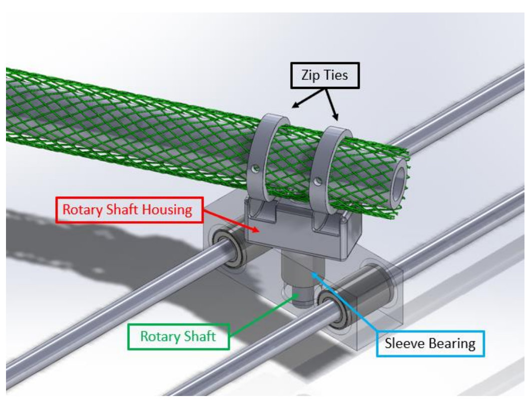

Figure 5. Detailed view of the assembly allowing for FAM rotation at the inlet ends. A sleeve bearing set into the translation carriage allows for rotation of a rotary shaft affixed perpendicular to the end of the FAM.

An eyehook design is incorporated into the end of the barbed plug used on the other end of the FAM. This hook facilitates rotation due to its round design and is attached to a dowel pin affixed to the central carriage. To account for the additional height gained from the attachment mechanism on the inlet end, 3D printed spacers are used to ensure both ends of the muscle fiber are held at the same height to prevent out-of-plane motion. 3D printed caps ensure the eye hook is fully constrained.

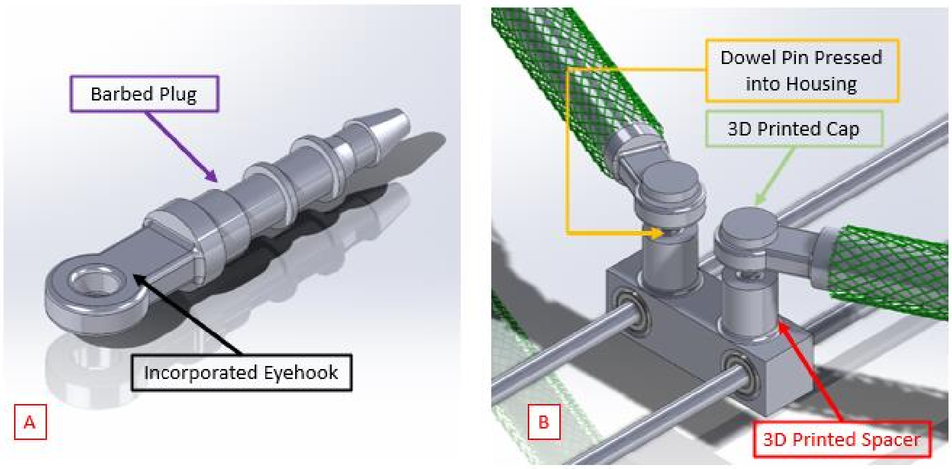

Figure 6: Detailed view of the rotational components at plugged ends of the FAMs. (a) model of the barbed plug used to fabricate the FAMs. (b) Detailed view of the attachment method used to secure the plugged fiber end to the testbed.

3.3 Pinned boundary condition considerations

The requirement that the outer ends of the pinned muscle fibers be fixed and unable to translate is realized in hardware through the use of locking shaft collars. The locking shaft collars are applied directly above and below the linear ball bearing housings to restrict their translation. The second requirement that the muscle fibers should not be in contact with each other for the duration of the test can be achieved by placing appropriately sized 3D printed spacers between the linear bearing housings.

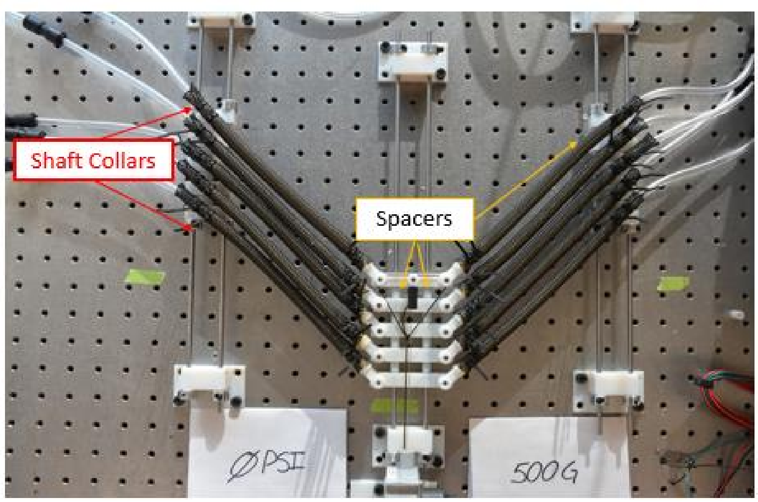

Figure 7: Pinned boundary condition implemented in hardware with 45° initial pennation angle. Shaft collars are located above and below the central carriages on the inlet end of the muscle fiber. Spacers are placed between the central carriages on both fiber ends.

3.4 Constant fiber contact boundary condition considerations

Prior to this study, the constant fiber contact boundary condition had not been implemented in an experimental setup. To achieve the constant fiber contact condition, the muscle fibers must begin in contact before actuation and remain in contact throughout actuation. To create the initial contact, the projection of the unpressurized outer diameter of the FAMs onto the vertical direction at the initial pennation angle must be at least as large as the depth of the linear bearing carriages. This requirement thus creates a relationship between the maximum depth of the linear bearing carriages and minimum initial FAM outer diameter, and minimum initial pennation angle for which the apparatus can exhibit the constant fiber contact condition. Spacers are not used for this configuration as the goal is to enable contact between the FAMs. The bottom pair of muscle fibers' inlet ends (located at the outer sides of be bundle) will have a fixed position that is defined by the presence of a locking shaft collar which acts as a stopper. The definition of this position assists in creating the pennation angle and ensuring that all radial expansion exhibited in the muscle bundle is harnessed in the same direction as the output motion.

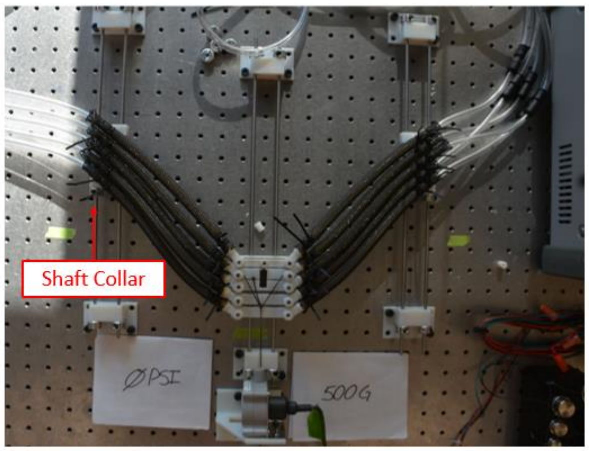

Figure 8: Constant fiber contact condition implemented in hardware with 45° initial pennation angle. Shaft collars are located on the linear rods below the carriages on the inlet end of the muscle fiber to assist in the creation of the pennation angle.

3.5 Muscle fiber fabrication

Ten artificial muscle fibers are fabricated using latex rubber tubbing with an outer diameter of 9.525 mm (⅜ in.) and an inner diameter of 6.35mm (¼ in.). The tubing is surrounded by braided mesh sleeving with an initial diameter of 9.525 mm (⅜ in.) and an expanded diameter of 12.7 mm (½ in.). The functional initial braid angle of this braided mesh is 37.7°. The target functional length was 165.1 mm (6.50in) with the average functional length being 165.35mm (6.51 in) and a range of ± 2.29 mm (0.09 in) from the target length. To reduce variability during testing, the same set of muscle fibers are used in both the pinned and the constant fiber contact condition experiments.

Table 1: Functional Length of Muscle Fibers

MUSCLE FIBER NUMBER	FUNCTIONAL LENGTH	MUSCLE FIBER NUMBER	FUNCTIONAL LENGTH
1	165.1 mm (6.50in)	2	166.11 mm (6.54 in)
3	164.08 mm (6.46in)	4	166.11 mm (6.54 in)
5	167.39 mm (6.59 in)	6	164.34 mm (6.47 in)
7	165.35mm (6.51 in)	8	163.83 mm (6.45 in)
9	165.1 mm (6.50in)	10	166.37 mm (6.55 in)

4. EXPERIMENTAL PROCEDURE

4.1 Experimental procedure

Using the testing platform described in Section 3, an experiment was conducted to determine the impact of varying pennate boundary conditions on the muscle bundle output. To achieve this, the setup was equipped with the 10 muscle fibers described in Section 3.5. The pinned and constant fiber contact boundary conditions were experimentally tested using prescribed pressures and loading conditions to experimentally determine their effect on contraction and pennation angle.

Pneumatic pressure was applied to the FAMs and controlled using a general purpose air pressure regulator. Actuation was achieved by supplying the FAMs with a set of predetermined pressures and allowing sufficient time to pass such that the pressure could be assumed to be constant throughout the muscle bundle at the time of data collection. Discrete pressures of 0 kPa , 68.95 kPa (10psi), 137.90 kPa (20 psi), 206.84 kPa (30 psi), 275.79 kPa (40 psi), and 344.74 kPa (50 psi) were supplied to the muscle bundle.

A Measurement Specialties SP2-250 string potentiometer affixed to the linear bearing carriage of the top pair of muscle fibers is used to determine the position of the muscle output point. The string potentiometer has a position measurement resolution of ± 0.25% of the collected measurement. Data was gathered using a NI PXIe-1078 and LabView Controller. The first 2000 data points sampled at 20k Hz were averaged to determine the muscle bundle position.

Loading was achieved using laboratory weights which were suspended in such a way that the force acted in a direction opposing motion. The minimum load applied is determined by the 1.9N ± 25% cable tension of the position measurement device. Additional loading was achieved by hanging precision weights from the top pair of muscle fibers to achieve a desired loading condition. The prescribed masses were 100g, 200g, 500g, 1000g, 1250g, 1500g, 1700g, 2000g, 2500g, 3000g, and 3500g precision calibration weights. Muscle bundle position data was gathered for each loading condition in 68.95 kPa (10 psi) pressure increments.

Using the data collected from the string potentiometer, the displacement of the muscle bundle was determined. To calculate the displacement, a point of zero contraction was defined as the point at which the muscle fibers experienced no added load (only the 1.9N from the potentiometer) and were unpressurized (0 kPa). The difference between the position data gathered at a specified operating condition and the point with zero contraction is defined as the displacement. This relationship is quantified in Equation 1.

$$\Delta Y = Y_{load} - Y_0 \tag{1}$$

For the purposes of this study, two types of displacement are defined. Contractile displacement is seen when the force exerted by the muscle bundle is sufficient to overcome the load force and the displacement observed is positive. Extensile displacement occurs when the loading of the muscle bundle is too great for the muscle bundle to contract above the point of zero contraction. Instead, the muscle bundle's experiences extensile deflection due to the elastic behavior of the muscle fibers which results in a negative displacement using Equation 1.

To quantify the rotation of the individual muscle fiber during actuation, an overhead camera recorded the instantaneous pennation angle that the muscle bundle experienced at all pressures and loading conditions. This pennation angle was measured from the images using a digital image analysis tool (https://www.ginifab.com/feeds/angle_measurement/) with a resolution of 1°. The initial pennation angle was measured as the angle at which the muscle fibers naturally rest in an unpressurized state with only the loading from the string potentiometer device. Because the length of the muscle fibers was held constant, initial pennation angle was varied by changing outer connection points to vary the thickness of the pennate muscle bundle and thus the pennation angle.

The pennation angle was measured from the images to determine the angle between the bottom muscle fiber and the vertical as seen in Figure 9. As the pressure was increased for the same loading condition, the muscle bundle would contract causing a change in pennation angle. This change is shown in the variation between images A,B, and C in Figure 9. This method was used to obtain the pennation angle for each loading condition and pressurization state.

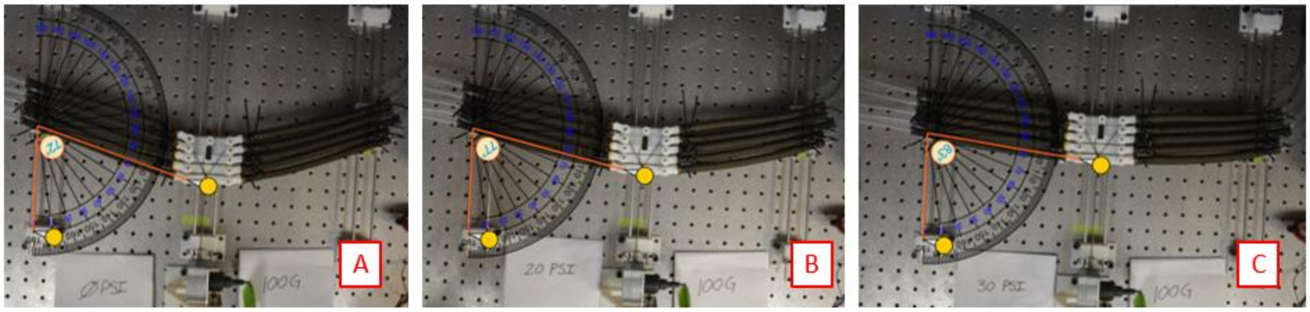

Figure 9. Pennation angle measurement method using digital image analysis for constant fiber contact boundary condition with 72° initial pennation angle, 2.88N load, and applied pressures of (A) 0 kPa (B) 137.9 kPa (C) 206.85 kPa

5. RESULTS

Using data obtained from the potentiometer, load vs. displacement plots were generated for varying initial pennation angles and boundary conditions. These results are shown in Figure 11. The error bars represent the minimum and maximum values seen in the averaged data set and the maximum variation in position from the potentiometer measurement. The starting pennation angles were approximately 45°, 57°, and 72° with a variation of ± 1°.

The blocked force, point of maximum contractile displacement, and point of maximum extensile displacement (shown in Figure 10 for an example case) are used to compare the behavior of the muscle bundle operating under varying boundary and loading conditions. The blocked force of the muscle bundle is defined to be the value at which the applied loading results zero displacement of the muscle bundle. The force required to displace the bundle 0 mm is estimated by fitting a curve to the obtained data points. The point of maximum contractile displacement is the maximum positive displacement obtained which is characteristically at the lowest applied load.

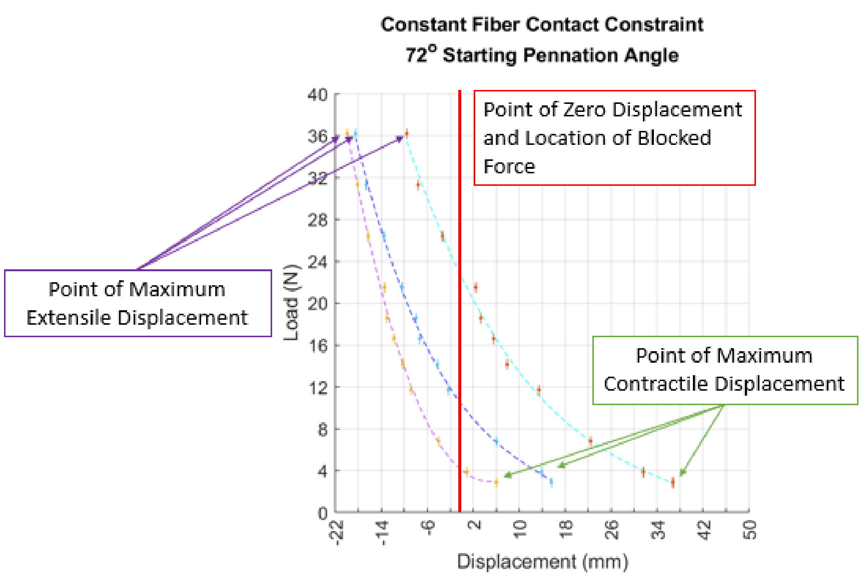

Figure 10. Locations of zero displacement, maximum contractile displacement, and maximum extensile displacement shown using the constant fiber contact constraint operating at a 72° initial pennation angle

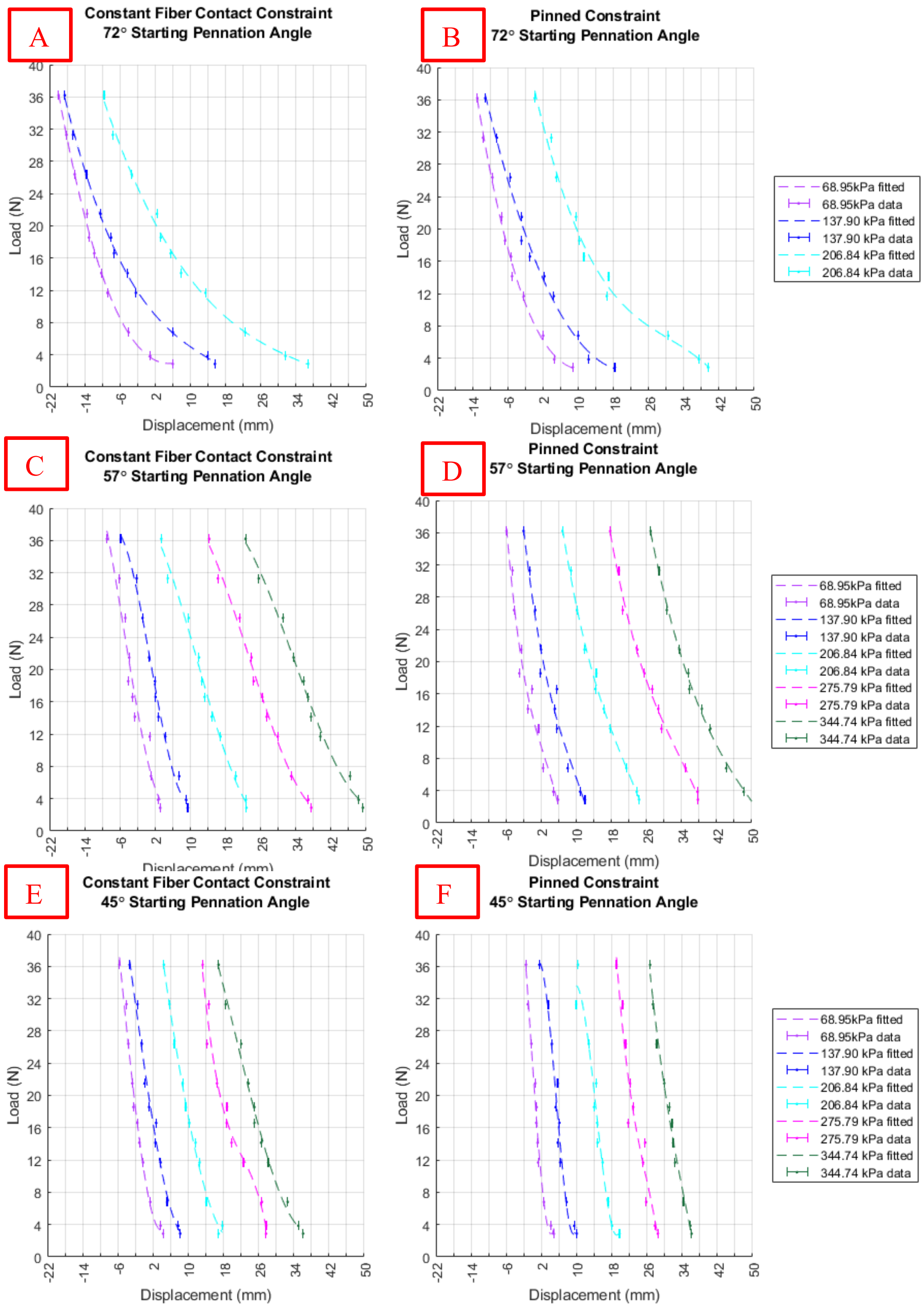

Figure 11. Force vs displacement plots for the following boundary conditions and starting pennation angles: (A) Constant fiber contact with 72° initial pennation angle; (B) Pinned condition with 72° initial pennation angle; (C) Constant fiber contact with 57° initial pennation angle; (D) Pinned condition with 57° initial pennation angle; (E) Constant fiber contact with 45° initial pennation angle; (F) Pinned constraint with 45° initial pennation angle

5.1 Pennation angle and blocked force

As the direction of the forces applied by the muscle fibers changes with pennation angle, the component of force in the direction of muscle motion (vertical in this experiment) varies. It is expected that as the pennation angle increases the blocked force will decrease due to the reduction of the output force component being directed along the line of motion. The number and parameters of the muscle fibers in the pinned and constant fiber contact boundary condition cases are held constant and thus the expected output force is expected to be constant between the two conditions for the same initial pennation angle. The validity of this assumption is determined by curve fitting the load-displacement data to estimate the blocked force (see table 2). This curve fit showed a reduction in estimated blocked force as the pennation angle increased for the pinned and constant fiber contact case. This reduction aligns with the expected behavior of a muscle bundle operating at an increased pennation angle. However, the boundary condition appears to have an impact on the relationship between reduction in blocked force and the increasing pennation angle.

Table 2. Estimated blocked force of the muscle bundle for a specified pressure obtained from fitting a curve to the collected data. If the curve fitted to the collected data did not cross the zero-displacement line, the blocked force is not extrapolated.

	Constant Fiber Contact Constraint			Pinned Constraint		
Pressure	45°	57°	72°	45°	57°	72°
68.95 kPa	9 N	9 N	4 N	23 N	13 N	8 N
137.90 kPa	22 N	23 N	10 N	--	27 N	17 N
206.84 kPa	--	--	23 N	--	--	36 N
275.79 kPa	--	--	--	--	--	--
344.74 kPa	--	--	--	--	--	--

For the constant fiber contact condition, the blocked force exhibits a large reduction between the 72° and 57° blocked force (as seen in figure 11.A, 11.C, and Table 2). This reduction is not seen in the blocked force data from figure 11.C and 11.E which compares the 57° and 45° initial pennation angles. Instead, the constant fiber contact condition appears to have approximately the same estimated blocked force when comparing the same pressures. This behavior illustrates constant fiber contact muscle bundles experience a large reduction in blocked force above a certain pennation angle.

The pinned boundary condition exhibits a trend that the blocked force will consistently decrease with increasing pennation angle. However, at largest tested pennation angle (72°) it should be noted that the estimated blocked force is shown to be more than 1.5 times the blocked force seen in the constant fiber contact case (Table 2). This high blocked force when compared with the constant fiber contact condition was also seen at the 45° pennation angle (Figure 11.E and Figure 11.F). However, at 57° the pinned case exhibits blocked force much more consistent with the constant fiber contact case with the average being an additional 4N produced by the pinned condition when compared with the constant fiber contact condition (Table 2).

The experimental results showed that the estimated blocked force follows different trends when under varying boundary conditions. This contrasts with the initial assumption that the blocked force is only related to the number, parameters, and applied pressure of the muscle fibers in the muscle bundle.

5.2 Pennation angle and displacement

The maximum and minimum loading conditions are used to determine the relationship between maximum muscle bundle output force and displacement. The displacement of the muscle bundle is affected by the length of the muscle fibers and their maximum contraction. The achieved displacement is also a function of the height and thickness of the muscle bundle. The initial pennation angle is the measurable result of these three factors. Previous studies have shown that for pinned configuration pennate muscle bundles the maximum contractile displacement depends heavily on the initial pennation angle and loading condition[10]. It is expected that the constant fiber contact constraint will exhibit the same behavior and produce more contractile displacement due to the radial expansion of the muscle fiber. To explore this trend, experimental displacement data for 206.84 kPa (30 psi) pressure will be used to compare the pennation angle data.

At low loads, the 72° starting pennation angle exhibits the maximum contractile displacement for both boundary conditions with the pinned constraint achieving a displacement value of 40mm and the constant fiber contact constraint achieving a displacement value of 37mm (seen in figure 11.A and 11.B). As the initial pennation angle decreased, the contractile displacement of the pinned configuration becomes 24mm and the constant fiber contact reduces to 23mm for the 57° initial pennation angle (figure 11.C and 11.D). At the 45° initial pennation angle the pinned condition achieves 20 mm contractile displacement while the constant fiber contact achieves 18mm (figure 11.E and 11.F). These trends demonstrate that the ability to approach full rotation increases the displacement value of the muscle bundle.

As load increases, the ability to achieve a high pennation angle is greatly impacted because of the changing direction of the force components. When applying high initial pennation angles, the rotational ability of the muscle bundle is dictated by the applied load. Figure 12 illustrates how high load impacts the maximum achievable pennation angle When comparing the change in pennation angle for the pinned and constant fiber contact boundary conditions figure 12 shows that for the 72° pennation angle there is little variation between the boundary conditions.

The low variation in pennation angle data between boundary conditions is also observed at lower initial pennation angles. However, figure 12 shows the impact of load on muscle bundles with low initial pennation angles is minimal when compared with the behavior of the 72° initial pennation angle case. Because pennation angle and displacement are related, this means that for a specified pressure, lower pennation angles can provide consistent displacement for a wide range of loads, while high pennation angles can provide high displacement for a small range of low loading conditions. This conclusion is strengthened by the plots in figure 11 which demonstrate that as pennation angle decreases the range of displacement for a specified pressure also decreases.

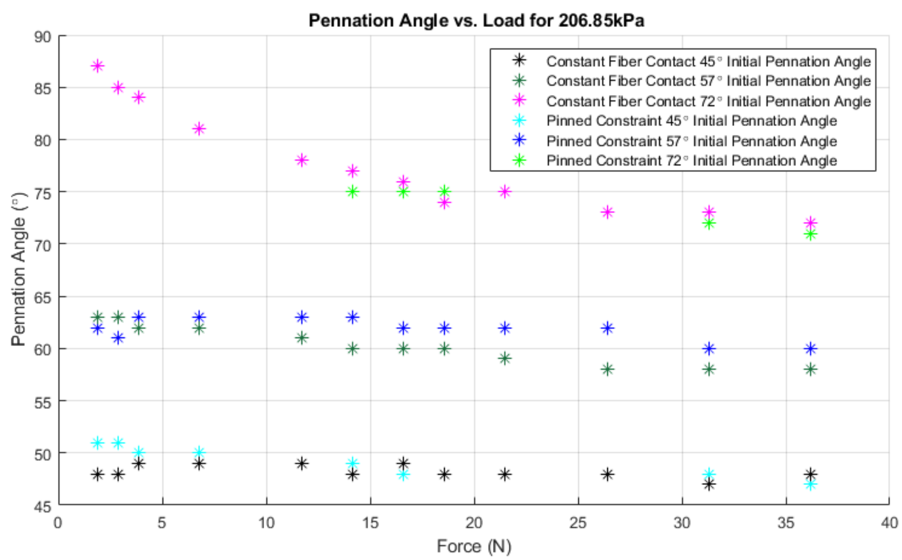

Figure 12. Relationship between the pennation angle and response to applied loading. Datapoints which overlap are displayed as a single point.

The bioinspired constant fiber contact condition was hypothesized to be capable of producing more contractile muscle displacement than the pinned configuration because fiber radial expansion (in addition to axial contraction) could contribute to the output motion of the muscle through the fiber contact and sliding ends. However, the observed contractions of the two boundary condition cases were similar and favored the pinned condition in some cases. Figure 12 illustrates that there is little variation between pennation angles due to imposed boundary conditions. However, at low pressures, the pinned constraint achieved up to 3mm of additional contraction when compared to the constant fiber contact condition (Seen in comparing Figure 11.C and 11.D). However, as higher pressures (above 206.84 kPa) are applied the variation in displacement is reduced to ± 1 mm. These observations suggest that, for the experiments performed, losses due to inter-fiber friction forces or deformation of the fiber cross sections when the fibers are in contact may dominate over additional contributions due to fiber radial expansion in the muscle output direction.

5. CONCLUSIONS

This paper outlines the effect of implementing pinned and constant fiber contact boundary conditions to bipennate McKibben artificial muscle bundles. The conditions of each boundary condition were defined and the considerations for implementing each in hardware were discussed. A testbed capable of imposing both boundary conditions on a bipennate muscle bundle operating at various pennation angles was constructed.

Using experimental data measuring the force output and displacement of the muscle bundles, relationships between the blocked force and displacement were determined for both boundary conditions and pennation angles of 45°, 57°, and 72°. The force output was shown to be decreasing as pennation angle increased and the constant fiber contact condition experienced a dramatic reduction in blocked force at 72° with little variation between the 45° and 57° pennation angles. The pinned case had a consistent reduction in blocked force as pennation angle increased.

Analysis of displacement data revealed that larger pennation angles (72°) can exhibit higher contraction at low loads than lower pennation angles. As the pennation angle decreases the displacement also decreases and the displacement values exhibit less variation for a larger range of values. The pinned boundary condition produced larger displacement values than the constant fiber contact condition despite the constant fiber contact condition's ability to harness displacement from radial expansion.

Future studies should investigate the effects of higher supplied pressures, muscle stiffness, and the effect on constant fiber contact muscle bundle output. The effects of friction and deformation in the constant fiber contact condition should be investigated and modeled. Additional theoretical and experimental investigation of this behavior would provide insight on the tradespace between boundary conditions.

REFERENCES

[1] Duan, E. and Bryant, M., "Design of Pennate Topology Fluidic Artificial Muscle Bundles Under Spatial Constraints," presented at ASME 2021 Conference on Smart Materials, Adaptive Structures and Intelligent Systems, 20 October 2021, American Society of Mechanical Engineers Digital Collection.

[2] Van Ham, R., Sugar, T., Vanderborght, B., Hollander, K. and Lefeber, D., "Compliant actuator designs," Robot. Autom. Mag. IEEE **16**, 81–94 (2009).

[3] Liang, W., Liu, H., Wang, K., Qian, Z., Ren, L. and Ren, L., "Comparative study of robotic artificial actuators and biological muscle," Adv. Mech. Eng. **12**(6), 1687814020933409 (2020).

[4] Tondu, B. and Lopez, P., "Modeling and control of McKibben artificial muscle robot actuators," IEEE Control Syst. Mag. **20**(2), 15–38 (2000).

[5] Bryant, M., Meller, M. A. and Garcia, E., "Variable recruitment fluidic artificial muscles: modeling and experiments," Smart Mater. Struct. **23**(7), 074009 (2014).

[6] Gentry, M. F. and Wereley, N. M., "Effects of Braid Angle on Pneumatic Artificial Muscle Actuator Performance," Smart Mater. Adapt. Struct. Intell. Syst. Vol. 2, 617–623, ASMEDC, Ellicott City, Maryland, USA (2008).

[7] Kim, J. Y., Mazzoleni, N. and Bryant, M., "Modeling of Resistive Forces and Buckling Behavior in Variable Recruitment Fluidic Artificial Muscle Bundles," 3, Actuators **10**(3), 42 (2021).

[8] Lee, H. J., Lee, K. H., Lee, Y. M., Choi, H. R., Moon, H. and Koo, J. C., "A bundled staggering patterned pneumatic muscle actuator for improved working efficiency," J. Mech. Sci. Technol. **33**(10), 4981–4989 (2019).

[9] Wakimoto, S., Suzumori, K. and Takeda, J., "Flexible artificial muscle by bundle of McKibben fiber actuators," 2011 IEEEASME Int. Conf. Adv. Intell. Mechatron. AIM, 457–462 (2011).

[10] Jenkins, T. and Bryant, M., "Pennate actuators: force, contraction and stiffness," Bioinspir. Biomim. **15**(4), 046005 (2020).